

# MEASUREMENTS OF RADIATION EXPOSURE ON COMMERCIAL AIRCRAFT WITH THE LIULIN-3M INSTRUMENT

E.G. Stassinopoulos<sup>1</sup>, C.A. Stauffer<sup>2</sup>, T.P. Dachev<sup>3</sup>, G.J. Brucker<sup>4</sup>, B.T. Tomov<sup>3</sup>, P.G. Dimitrov<sup>3</sup>

## Abstract

This paper reports on the development of a compact radiation monitor/dosimeter, the LIULIN-3M, and on extended measurements conducted on the ground and on commercial aircraft on domestic and international flights.

## Introduction

The LIULIN-3M radiometer evolved from an international cooperative project by a group of Bulgarian, Russian, German, and American Scientists. The radiometer is a low power, small size, light weight, and low cost instrument composed of a solid state detector (SSD) with supporting electronics that enable it to operate as a pulse height analyzer of energy deposited in the detector, and to obtain from these measurements the total dose or the dose rate produced by charged particles. A flash memory allows self-storage of data during flights and post flight retrieval [1,2,3,4].

## Description

The basic detector is a Silicon-Lithium Drifted diode, 1 mm thick, with a sensitive area of 1 cm<sup>2</sup>, and a weight of 0.232 g. Figure 1 contains a block diagram that shows the supporting electronics. Charge pulses generated from the energy deposited by incident particles are passed to the charge sensitive amplifier, then to the discriminator and peak hold detector, and finally, they are converted from analog to digital signals by the 8-bit ADC ( Analog-to-Digital Converter) and sorted into 256 channels, according to their voltage amplitudes. Two microprocessor units manage the data flow to and out of the memory devices.

The specifications and dynamic ranges of the instrument are listed in Table 1. The energy deposited or loss in silicon by the incident particles ranges from 0.16 to 13.8 MeV. The measurement time per spectrum of the instrument can be varied from 30 s to 30 min.

---

<sup>1</sup> NASA Goddard Space Flight Center, Greenbelt, MD, 20771

<sup>2</sup> Stinger Gaffarian Technologies, Greenbelt, MD, 20771

<sup>3</sup> Bulgarian Academy of Sciences, Solar-Terrestrial Influences Lab, 1113 Sofia, Bulgaria

<sup>4</sup> Radiation Effects Consultants, Inc., West Long Branch, NJ 07764

**Table 1. Specifications and dynamic ranges.**

<u>Specifications</u>	<u>Ranges</u>
Mass: (including batteries) 960 g	Flux: 1 – 5000 part/cm <sup>2</sup> -s
Size: 140 x 80 x 30 mm <sup>3</sup>	Energy Deposited: 0.16 – 13.8 MeV
Temperature: -20°C to +45°C	LET: 0.16-13.8 keV/μ
Measurement Time: 30s to 30 min	

The LIULIN-3M operates in two modes, namely, “Working Mode” and “Data Transfer Mode”. In the Working Mode, the switch “ON” button connects the instrument via a jack to a polarized relay. In this mode the device is operating under the control of the program in the microprocessors to collect dose, flux, and spectra until the memory is filled. At that time, the instrument is automatically turned “OFF” through the relay. The total time spent in the Working Mode is 480 hours. The expected lifetime of the lithium batteries is about 1000 hours.

In the Transfer Mode the device is switched “ON” after it is delivered to the principal investigator. This mode allows the transfer of the accumulated data in the flash memory to a personal computer (PC) under a parallel port communication link. During this mode the data are correlated to the real time of the flight.

The major parameter of the instrument is the amplitude of the charge pulses generated in the solid state detector by the incident particles. They are then passed to the charge-sensitive amplifier that converts them to corresponding voltage pulses. The sensitivity or conversion factor of this pre-amplifier is 240 mV/MeV. These signals are subsequently amplified by a factor of 5 in the main amplifier stage. The threshold setting of the discriminator is 38.7 mV which establishes the lower data limit and consequently, the number of channels assigned to noise signals. Since there are 256 channels in the Analog-to-Digital converter and the upper voltage limit is 3.3 V, the sensitivity per channel is  $3.3/256 = 12.89$  mV/Ch and thus the first three channels are assigned to storing noise pulses. The deposited energy (Dep E) is given by equation (1):

$$\text{Dep E(MeV)} = \sum_i (\text{counts}_i * \text{channel}_i) * M \quad i = 4 - 256 \quad (1)$$

where the conversion factor M is given by:

$$M = \left( 12.89 \frac{\text{mV}}{\text{Ch}} \right) / \left( 240 \frac{\text{mV}}{\text{MeV}} \right) = 0.05371 \frac{\text{MeV}}{\text{Ch}} \quad (2)$$

and the corresponding dose rate per hour by:

$$\text{Dose Rate } D_R (\mu\text{Gy}_{\text{si}}/\text{h}) = K * \text{Dep E (MeV)} / t_c \quad (3)$$

where  $t_c$  is the collection time (in seconds) and the conversion factor  $K$  is:

$$K = 2.486 \text{ in units of } \mu\text{Gy}_{\text{si}} / \text{h} * \text{MeV} \quad (4)$$

## Results

All data presented herein were collected on commercial flights every five minutes but the conditions of the measurements were not systematically controlled, particularly in terms of location and altitude. Figure 2 is a plot of dose rate versus minutes after the instrument was turned on for a flight from Washington, D.C. to Los Angeles, CA, Figure 3 covers the trip from Los Angeles to Auckland, New Zealand, and Figure 4 shows the last leg of the flight from Auckland to Christchurch, NZ.

Figures 5, 6, and 7 represent plots of measurements for flights from Washington, DC, to Denver, CO, Denver to Houston, TX, and finally, Houston to Denver then back to Washington the same day, respectively. Figure 8 is a summary plot of these four flights. Figures 9 and 10 show data taken on flights from Washington, DC, to Paris, France, and also on the return flight.

Figure 11 contains a plot of the instrument's measurements of dose rate versus time after turn-on for the Sofia-New York flight, indicating the background at the airport and the three data points for which the altitude levels are given. Figure 12 contains a plot of the data showing a curve fit to the four available data points versus altitude. Figure 13 depicts the data for the flights from Washington to Budapest. The measurements obtained on the return flight segments are plotted in Figure 14.

In most of the commercial flights, altitude information was made available by the Airlines after the flights; however, for the trip from Sofia, Bulgaria, to New York, NY, altitude data were provided to members of the LIULIN team on-board the plane by the pilot on three occasions, while on a recent flight from Washington, DC, to Frankfurt, Germany, to Budapest, Hungary, flight information (latitude, longitude, altitude, speed, temperature) was continuously presented on TV monitors in the cabin. It should be noted, however, that for some flights altitude data could not be obtained.

## Discussion

For all flights reported in Figures 2 to 14, the peak dose rates are a function of two variables: altitude and magnetic latitude. Thus, in Figure 2 for the trip from Washington to Los Angeles the peak rate reached almost  $0.2 \mu\text{Gy}/5\text{-min}$ , whereas in Figure 3 for the trip from Los Angeles to Auckland, the dose rate remained around  $0.07 \mu\text{Gy}/5\text{-min}$  for

the major part of the flight over the Pacific Ocean, and only climbed to a peak of about  $.12 \mu\text{Gy}/5\text{-min}$  near the end of the trip (last 2.5 hours). The dose rate for the short flight from Auckland to Christchurch, Figure 4, peaked at about  $0.09 \mu\text{Gy}/5\text{-min}$ .

In this context, particularly interesting are the measurements from the Los Angeles to Auckland flight, shown in Figure 3. The low dose rates would imply a correspondingly low altitude, perhaps 30000 feet, but the airline confirmed that this specific flight took place at an altitude of 39000 feet.

These measurements confirm that, as expected, flights toward lower magnetic latitudes, that is toward the magnetic equator, will experience smaller doses. The reason is that only a few very high energy galactic cosmic rays (several GeV/nucleon) can penetrate to those regions of the globe on account of the earth's magnetic field which deflects most arriving particles with lower energies (rigidity concept). The low dose rates shown in Figure 3 are probably due to the shielding effects of the earth's magnetic field which compensated for the normally higher cosmic ray progeny distribution at the elevated altitude of this flight.

The peak rates during the two flights covered in Figures 5 and 6, Washington-Denver-Houston, were about  $0.15$  and  $0.13 \mu\text{Gy}/5\text{-min}$  respectively. During the return trip, however, the peak rates achieved a surprisingly high level of  $0.19 \mu\text{Gy}/5\text{-min}$  for the Houston-Denver segment and  $0.28 \mu\text{Gy}/5\text{-min}$  for the Denver-Washington segment, as shown in Figure 7. The summary of these four flights is shown in Figure 8. The altitude of the aircraft, as given to us at a later date by the airline, was highest on the Houston-Denver (35000 ft) and Denver-Washington flights (37000) compared to the Washington-Denver (35000 ft) and Denver-Houston (33000ft) flight. It remains to be determined why the short duration Houston-Denver flight at 35000 ft experienced a higher dose rate (by  $\sim 20\%$ ) than the Washington-Denver flight at the same altitude but of much longer duration.

Figures 9 and 10 show data for a trip to Paris, France, and return to Washington, D.C. respectively. The longer flight time of about 6 hours shows that the rate was about constant for the flight to Paris, approximately  $0.18 \mu\text{Gy}/5\text{-min}$ , but on the return to Washington a constant rise in rate is observed, with a peak of about  $0.23 \mu\text{Gy}/5\text{-min}$  at the end of the trip as shown in Figure 10. Since we have no reliable altitude information for these flights, it is difficult to interpret the data correctly.

The flight from Sofia to New York provided for the first time an opportunity to measure the variation of the instrument's response in real-time as a function of altitude through the cooperation of the pilot. Figure 11 shows a plot of dose rate versus time after turn-on. During the trip to New York the plane flew at three different altitudes of 31000, 35000, and 37000 feet. It can be seen that the detector measured three distinct dose rates. These three rates are plotted in Figure 12 versus altitudes, including the background rate on the ground. A curve fit was made to the four data points and extrapolated to 40000 feet where the dose rate approaches  $0.5 \mu\text{Gy}/5\text{-min}$ .

In Figures 13 and 14 for the trip to Frankfurt-Budapest and return, again a similar pattern was observed as that seen in Figures 9 and 10 for the Washington-Paris and Paris-Washington flights, namely the trips east to Paris (Fig. 9) and to Frankfurt (Fig. 13) indicate a relatively constant level of exposure rate during the transatlantic voyage, whereas both return trips west show a gradual increase in the dose rate as the flights progress. Assuming that the flight corridor is the same for both directions, it is conjectured that the variation is altitude dependent, that is, lower altitudes going east and gradually higher altitudes going west, maybe in consideration of the jet stream (?). This will be investigated and resolved for the final paper.

All figures show low "background" measurements on the ground before take-off and after landing, ranging from 0.017 to 0.033  $\mu\text{Gy}/5\text{-min}$ . Upon close examination it is apparent that the data from low altitude locations like Washington, Houston, and Los Angeles, with elevations less than 100 feet, have almost the same values as data from elevated locations as, for example, Snowmass, CO, at over 9000 feet altitude (see fig. 8), that is: average of about 0.0208  $\mu\text{Gy}/5\text{-min}$  and 0.0225  $\mu\text{Gy}/5\text{-min}$ , respectively. Since a noticeable difference in average dose rates should be observed at these two altitudes, the low elevation data may contain some level of instrument noise. The normal global average rate of radiation background levels, excluding high concentrations of naturally occurring radionuclides such as radium, thorium, uranium, etc., has been reported to be about 0.008 to 0.017  $\mu\text{Gy}/5\text{-min}$  at about 1 meter above ground and including cosmic ray contributions coming from above [5]. It has been established that the detector orientation has no discernible impact on the measurements, in flight or on the ground.

The total dose accumulation for each traveled flight segment will be calculated and presented in the full-length paper. As additional data are being accumulated over global distances with large longitudinal and latitudinal variations, a comparison to some predictions of cosmic ray intensities and their progeny may be possible, not only in terms of altitude but also as a function of rigidity and geomagnetic shielding affects.

## Conclusions

The LIULIN-3M instrument is an effective radiation monitor for aviation or space application. It is characterized by small size, low power, light weight, and low cost. The instrument is currently being used to perform global surveys of radiation environment levels within aircraft and on high-altitude balloon missions over the south pole (U.S. Antarctic Program). Measurements from a multitude of commercial airline flights conducted so far, indicate a strong altitude and magnetic latitude dependence, as predicted by theory. The maximum dose rate encountered until now is about 0.3  $\mu\text{Gy}$  per 5-minute interval.

## **Acknowledgement**

The authors wish to express their appreciation to UNITED AIRLINES for assisting in this research, with special thanks to Rick Koski, UNITED's shift manager at Washington's Dulles International Airport, for his valuable help in providing us with important altitude data for some past flights.

## **REFERENCES**

- [1] V.M. Petrov, V.S. Mahkmtov, N.A. Panova, V.A. Shurshakov, Ts. P. Dachev, J.V. Sekova, and Yu. P. Matvijchuk, "Peculiarities of the Solar Proton Events of 19 October 1989 and 23 March 1991 According to the Measurements Onboard the MIR Space Station", Adv. Space Res., Vol. 14, No. 10 pp (10) 645-(10) 650, 1994.
- [2] J.V. Semkova et al, "Experience from Active Dosimetric Investigations on MIR-Space Station. Proposal for a New Conception and Design of Space Dosimetry Systems for Future Manned Missions", 44<sup>th</sup> Congress of the International Astronautical Federation, Oct16-22, 1993/ Graz Austria.
- [3] J. Semekova et al., "Dosimetric Investigations on Mars-96 Mission", Adv. Space Res., Vol. 14, No. 10, pp. (10)707-(100719, 1994.
- [4] Ts. P. Dachev, B.T. Tomov, G. Georgiev, P.G. Dimitrov, Yu. N. Matviichuk, V.M. Petrov, V.V. Shurshakov, E.G. Stassinopoulos, and J. Bart, "Analysis of the Calibration Results of the Engineering Model of LIULIN-3 Radiometer-Dosimeter", Proceedings of the 3<sup>rd</sup> National Conference on Solar-Terrestrial Influences, II-73, Sofia, Bulgaria, June 1998. (In Bulgaria)
- [5] P.F. Gustafson and S.S. Brar, "Gamma-Emitting Radionuclides in Soil", The Natural Radiation Environment, Editors John A.S. Adams and Wayne H. Lowder, University of Chicago Press, 1964.

**FILE NAME:** measumnts of rad. Expos. on commrci aircraft.doc

**DATE:** (last updated) 7-29-99

**LOCATION:** c: Stass's Documents



## THE LIULIN-3M RADIOMETER BLOCK DIAGRAM

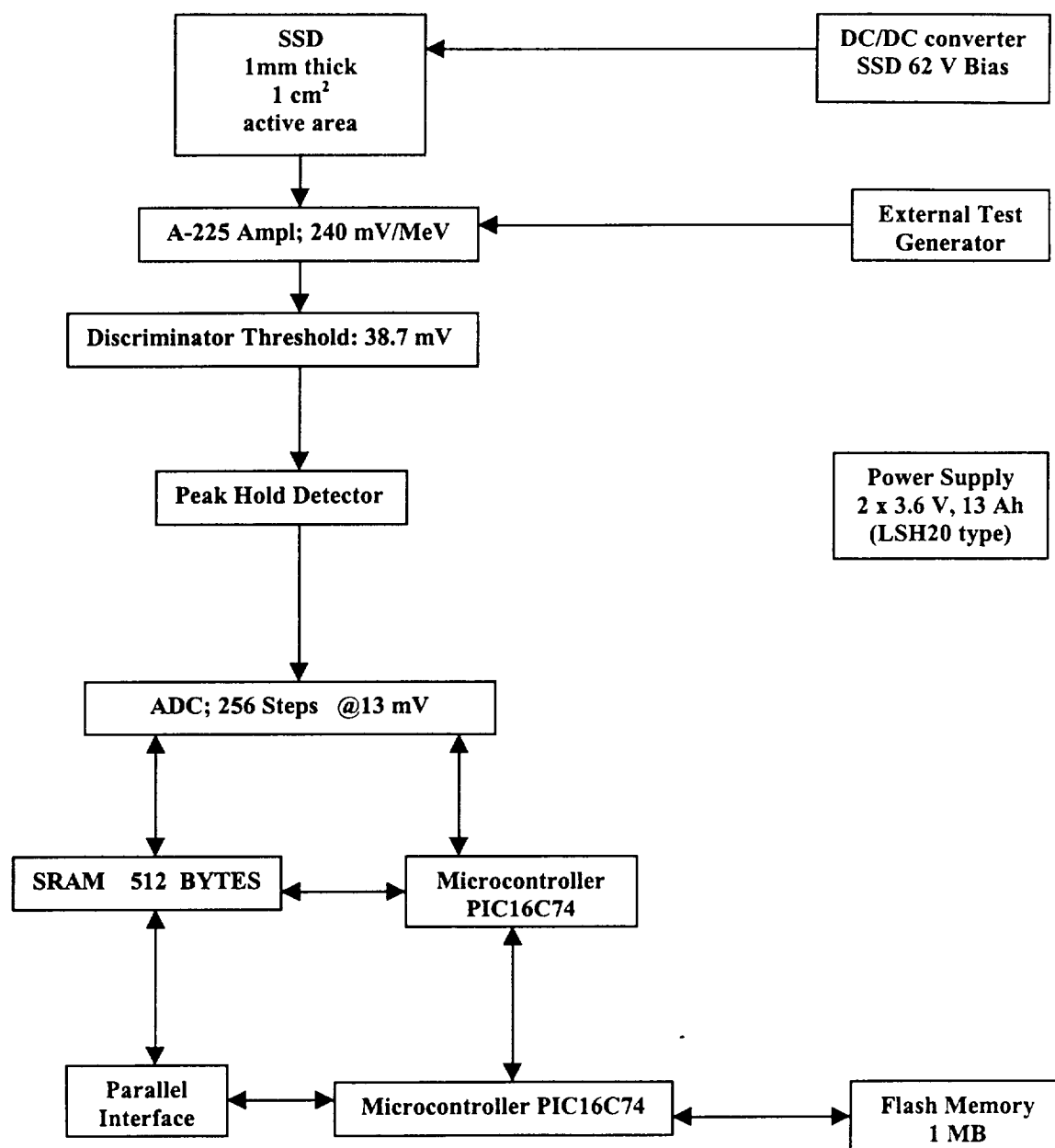


FIGURE 1

# Liulin-3M Commercial Flight Data

Washington, DC - Los Angeles, CA (12/7/97)

Channels 12 Through 256

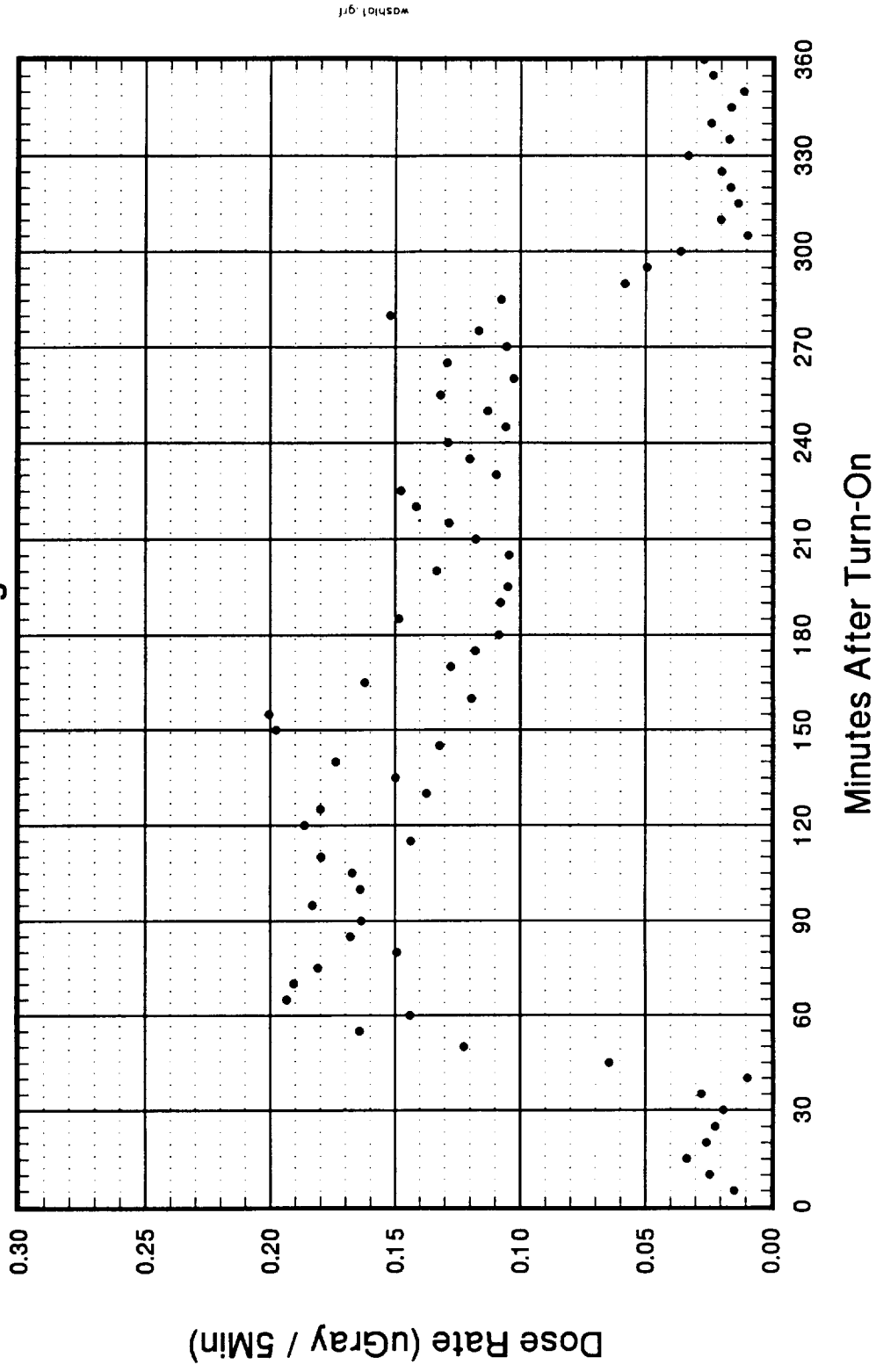


FIGURE 2

# Liulin-3M Commercial Flight Data

## Los Angeles, CA - Auckland, NZ (12/8/97)

Channels 12 Through 256

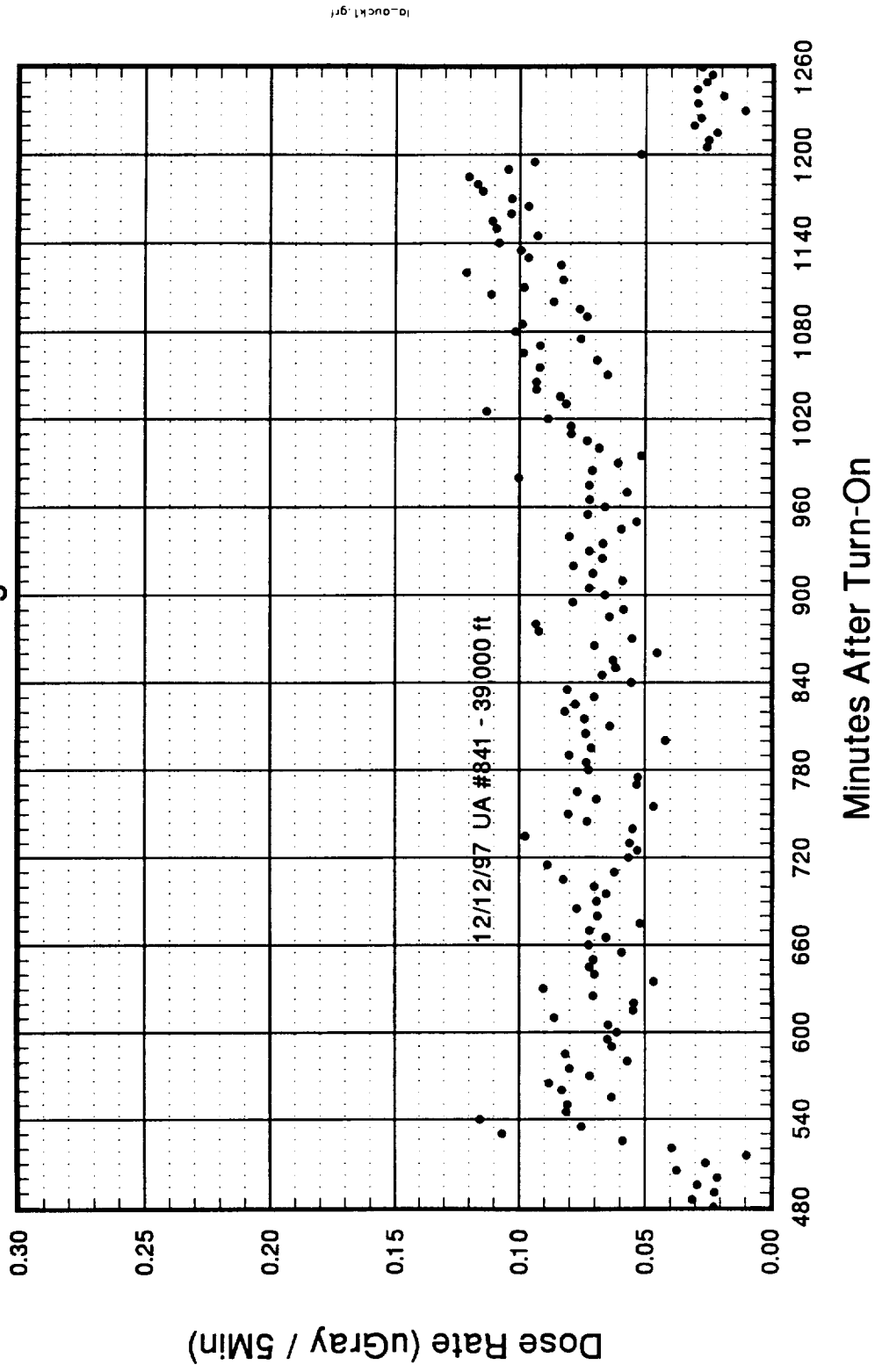


FIGURE 3

# Liulin-3M Commercial Flight Data

Auckland, NZ - ChristChurch, NZ (12/8/97)

Channels 12 Through 256

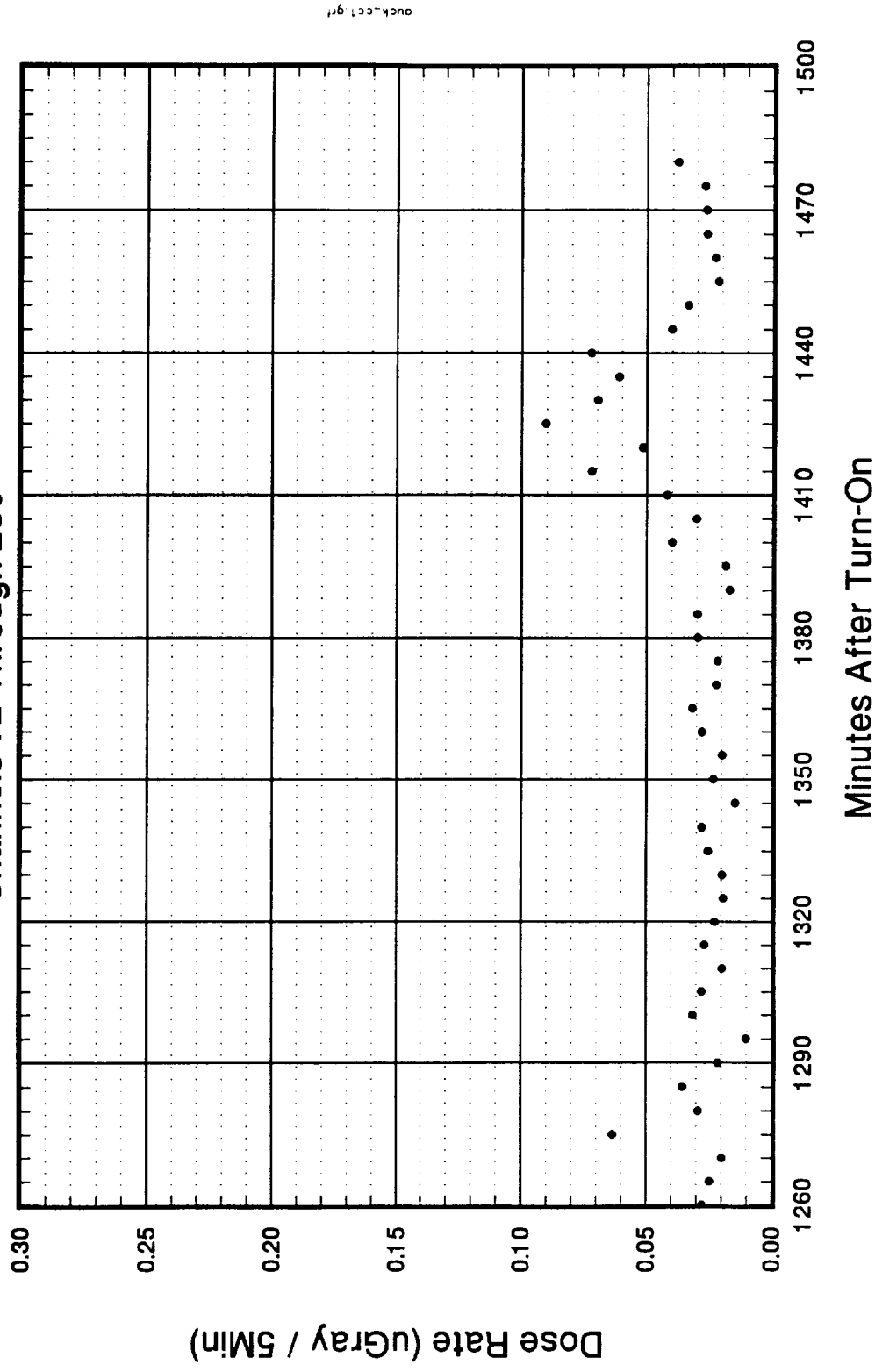


FIGURE 4

# Liulin-3M Commercial Flight Data

## Washington, DC - Denver, CO

Channels 12 Through 256

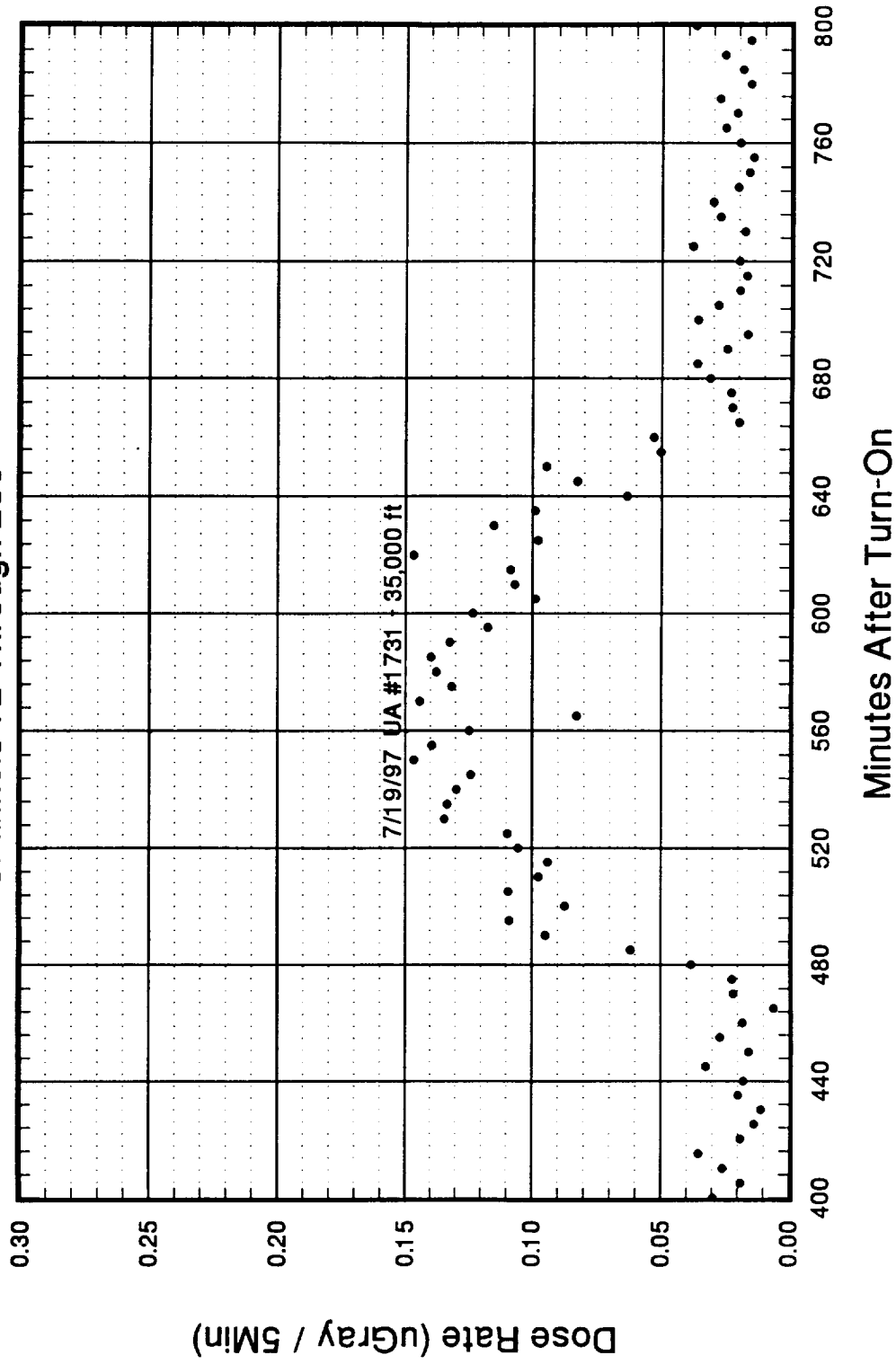


FIGURE 5

# Liulin-3M Commercial Flight Data

Denver, CO - Houston, TX

Channels 12 Through 256

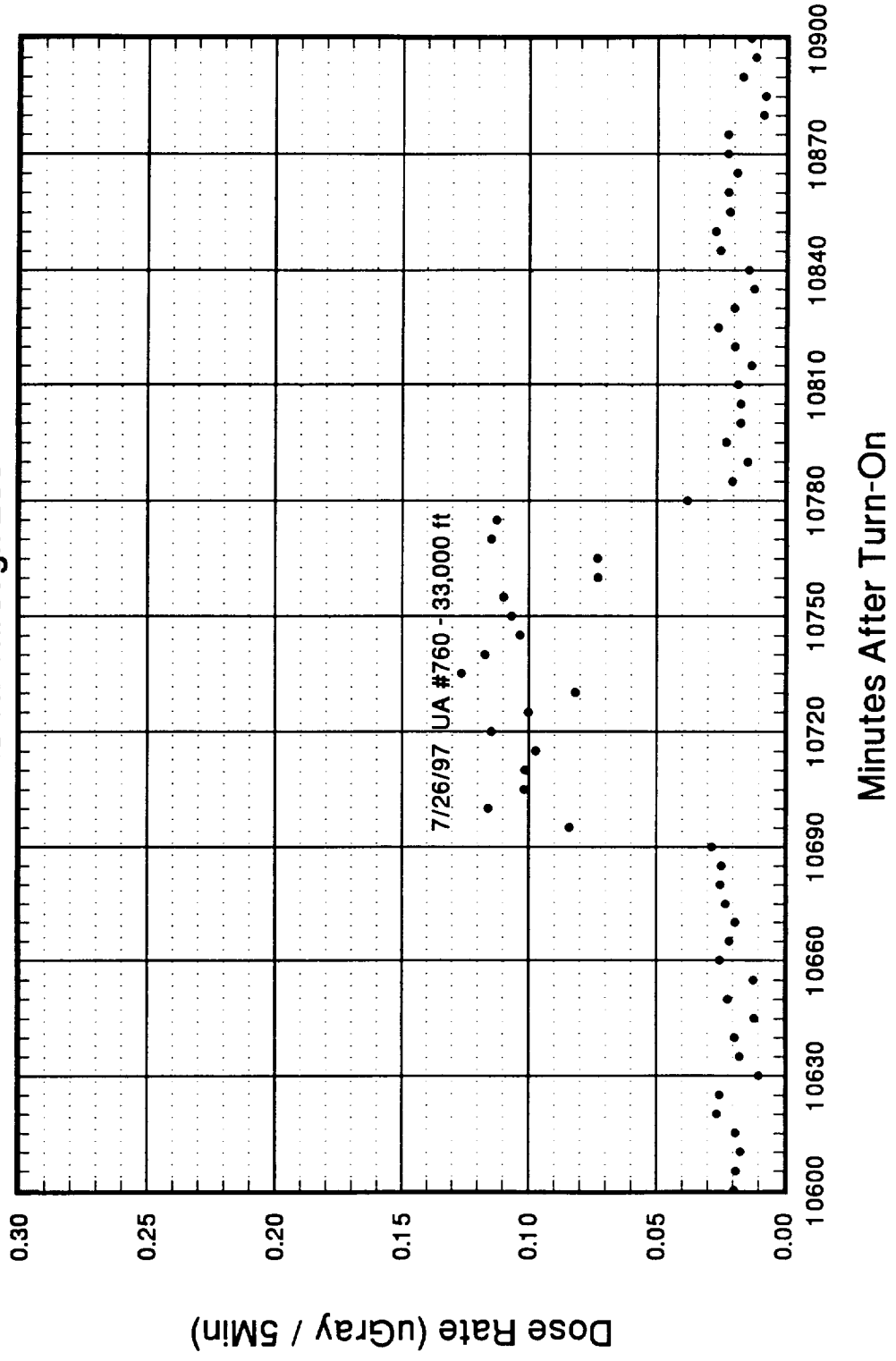


FIGURE 6

# Liulin-3M Commercial Flight Data

Houston, TX - Denver, CO - Washington, DC

Channels 12 Through 256

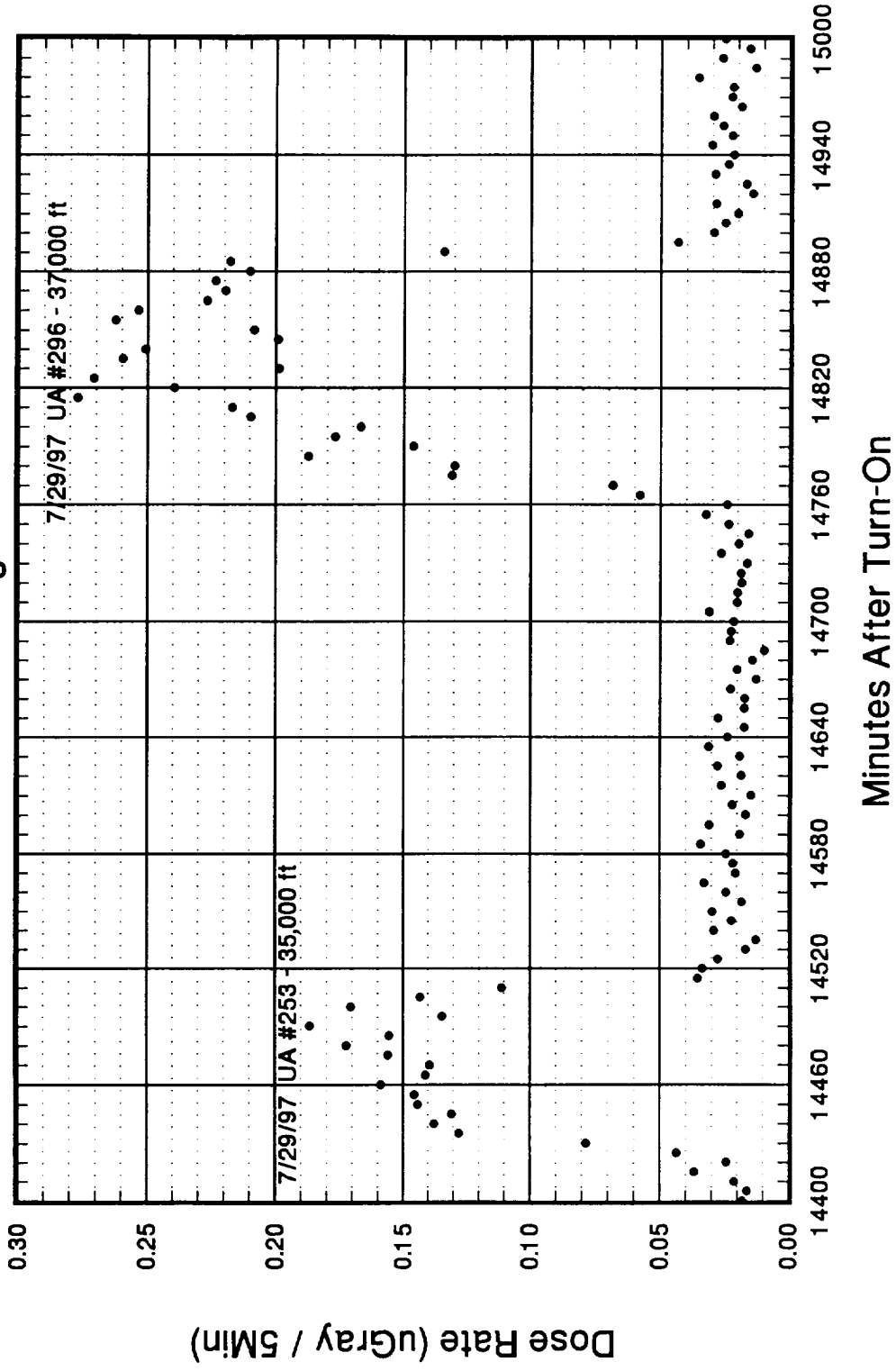


FIGURE 7

# Liulin-3M Commercial Flight Data

Washington, DC - Denver, CO - Houston, TX - Denver, CO - Washington, DC

Channels 12 Through 256

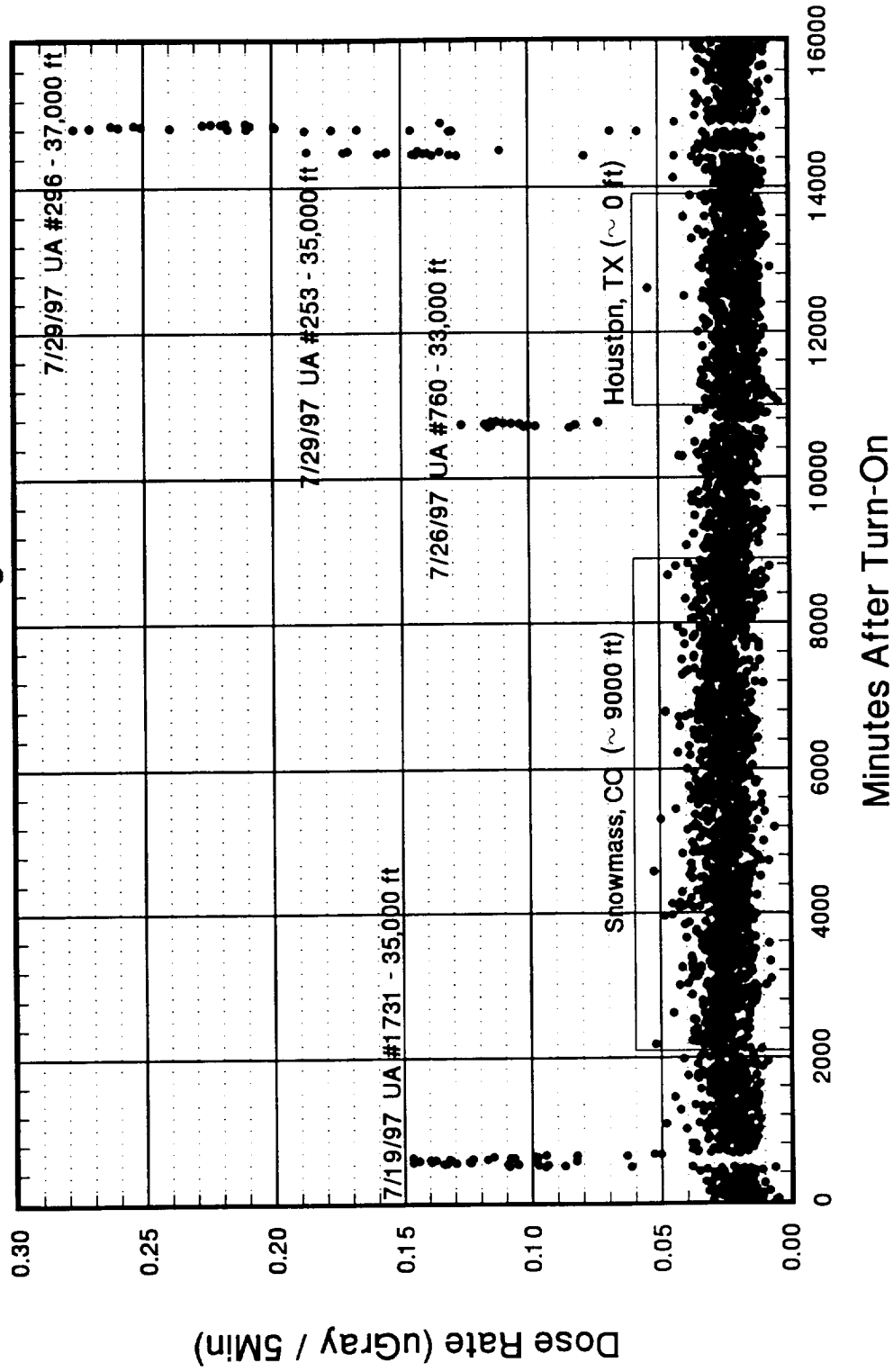


FIGURE 8



# Liulin-3M Commercial Flight Data

## Washington, DC - Paris, France (9/10/97)

Channels 12 Through 256

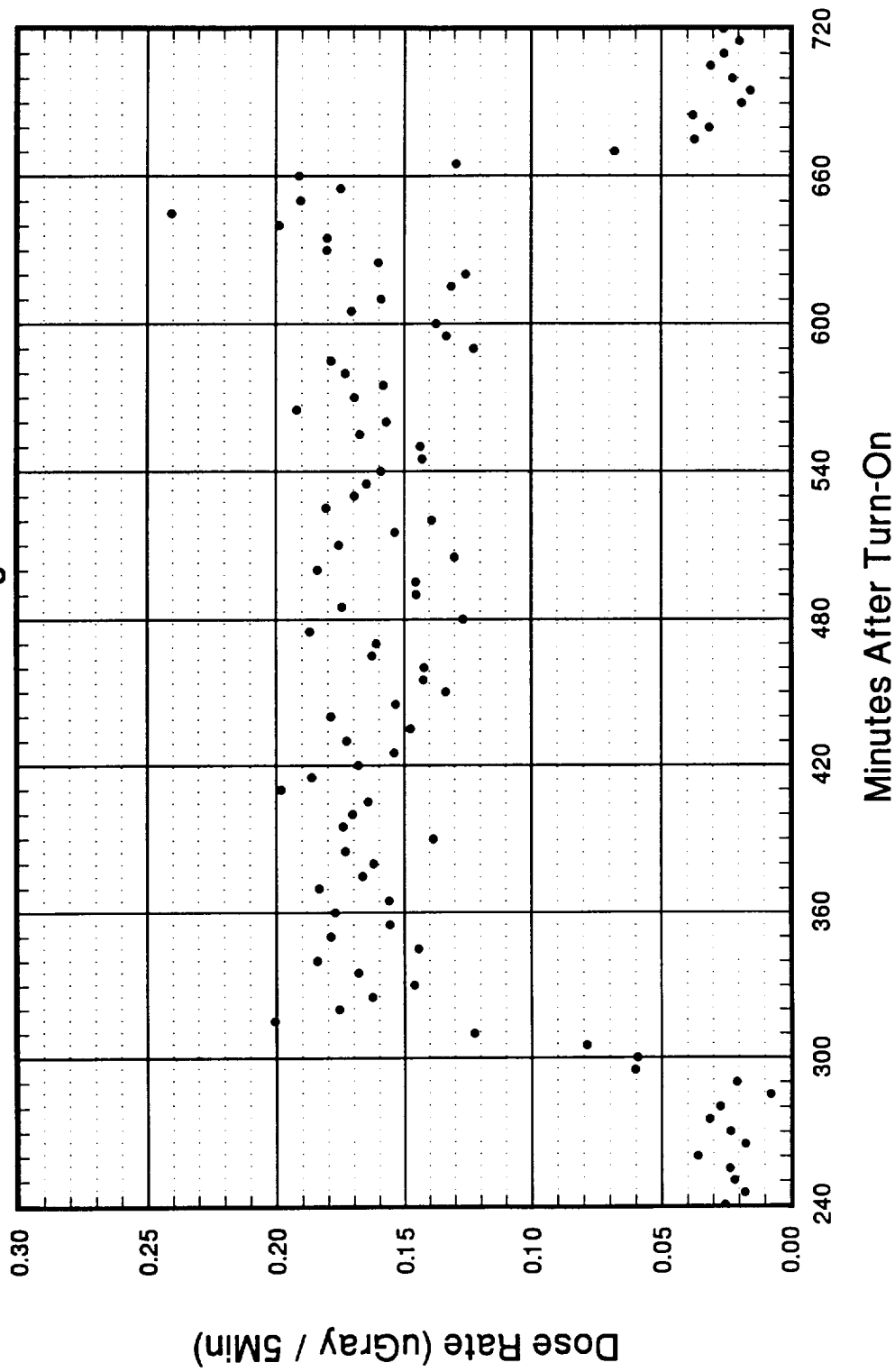


FIGURE 9

## Channels 12 Through 256



# FIGURE 10

# Liulin-3M Commercial Flight Data

Sofia, Bulgaria - New York, New York (6/16/97)

Channels 12 Through 256

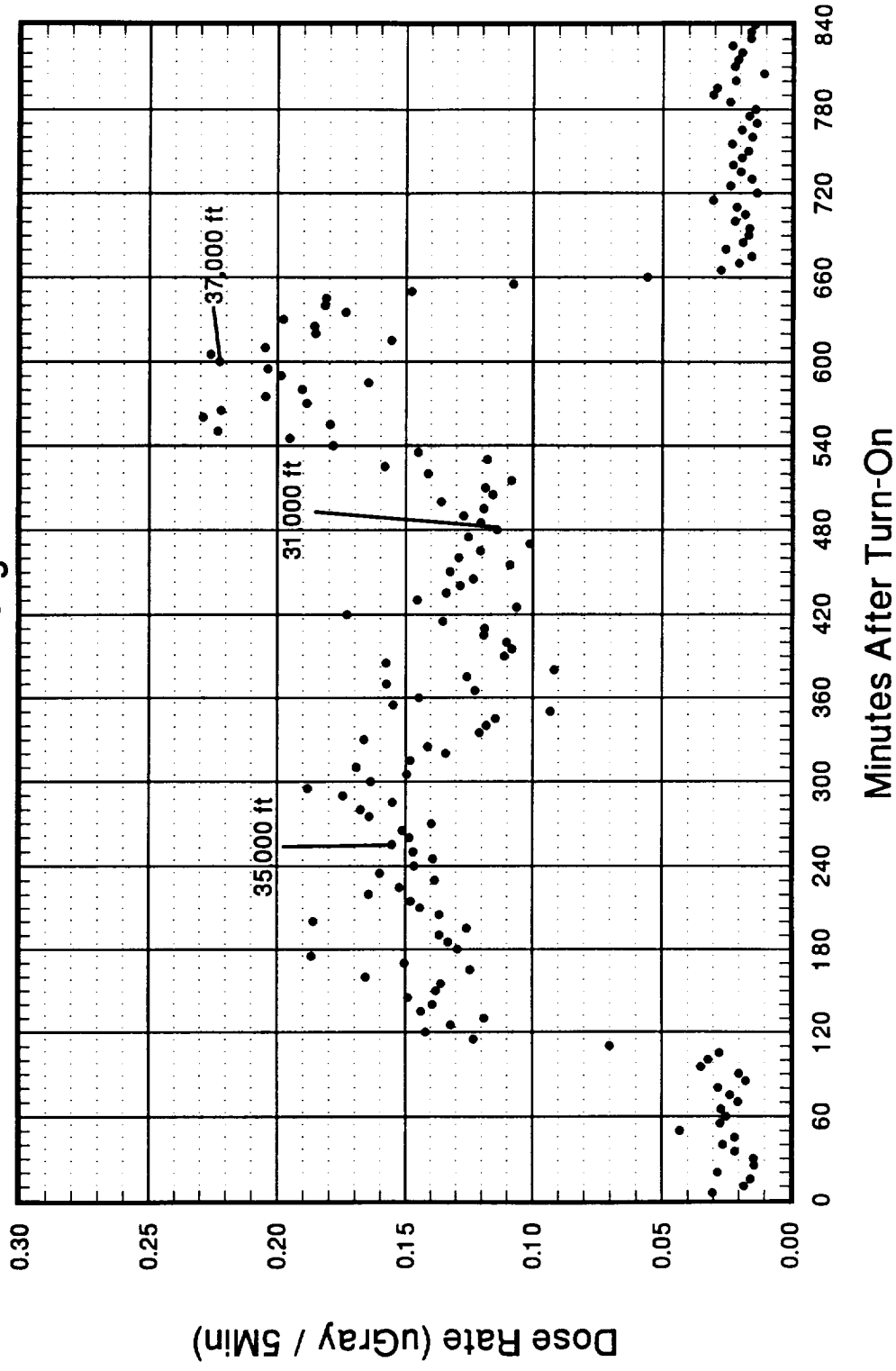


FIGURE 11

# Liulin-3M Commercial Flight Data

Sofia, Bulgaria - New York, New York

$$\text{Dose} = \{(2.8915 \times 10^{-4} + \text{Altitude} \times 7.8218 \times 10^{-8}) / (1 - \text{Altitude} \times 2.5223 \times 10^{-5})\}^{0.5}$$

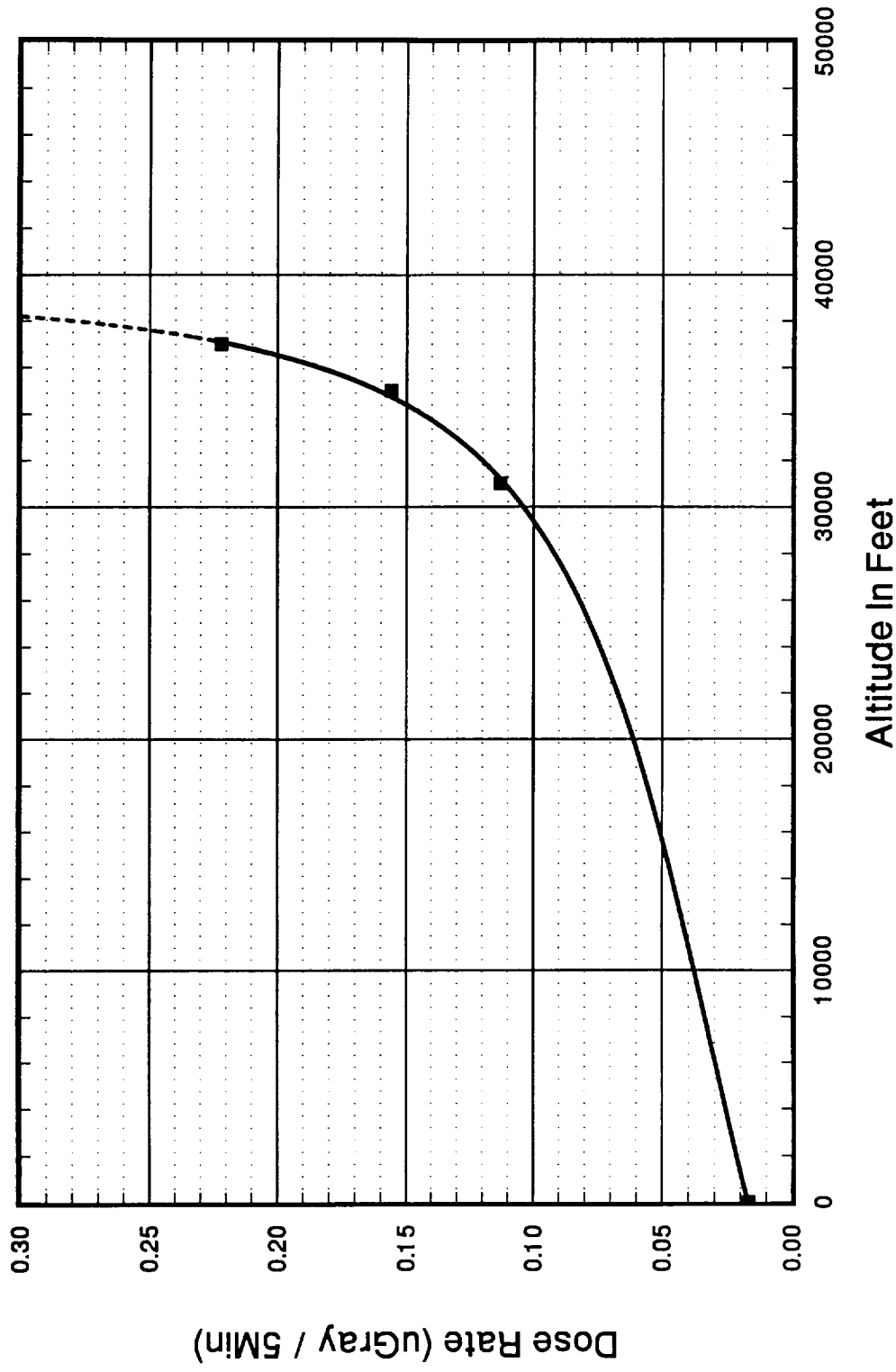


FIGURE 12

# Liulin-3M Commercial Flight Data

Washington, DC - Frankfurt, Germany - Budapest, Hungary (3/21/98)

Channels 12 Through 256

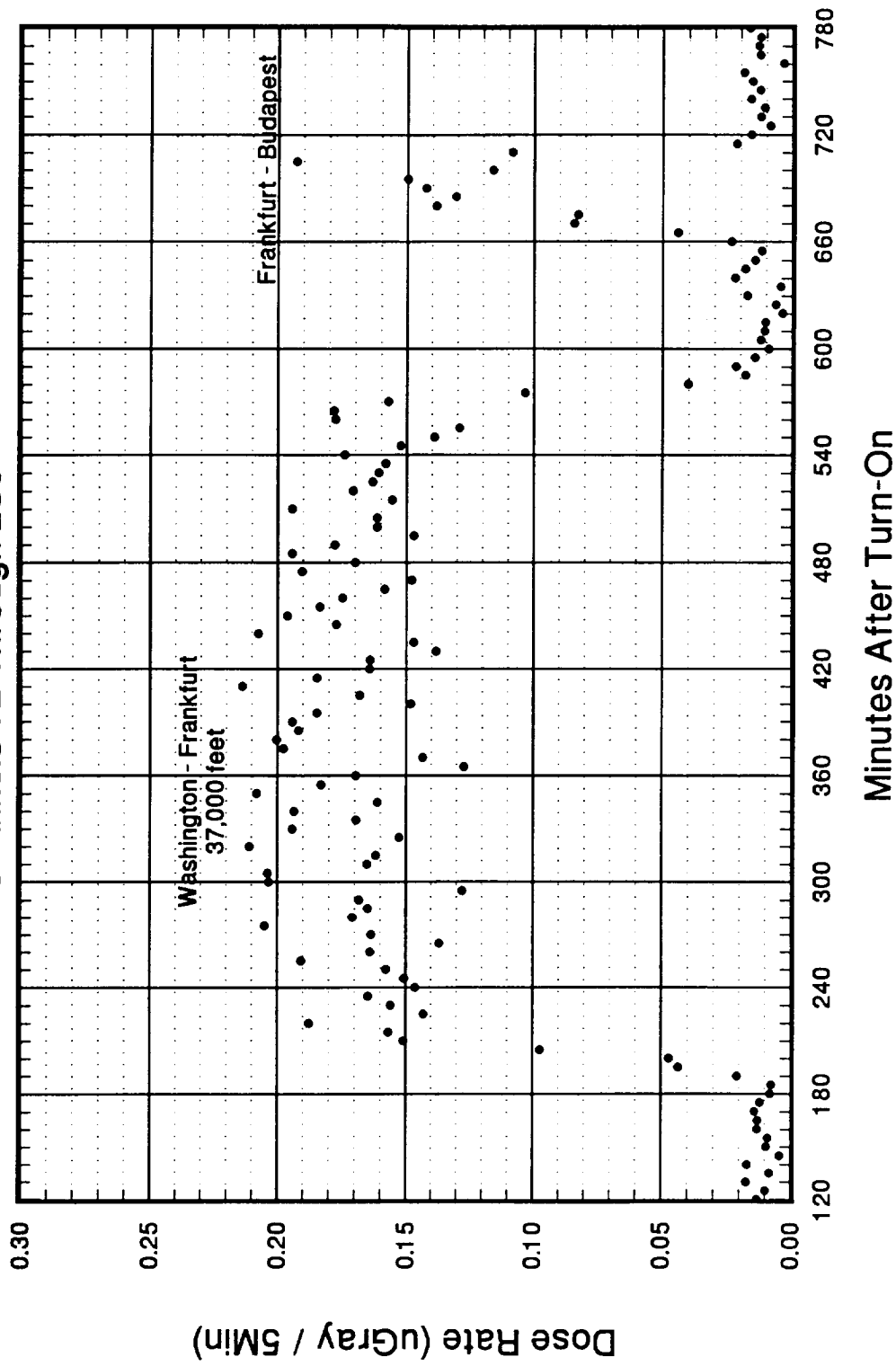


FIGURE 13

# Liulin-3M Commercial Flight Data

Budapest, Hungary - Frankfurt, Germany - Washington, DC (3/30/98)

Channels 12 Through 256

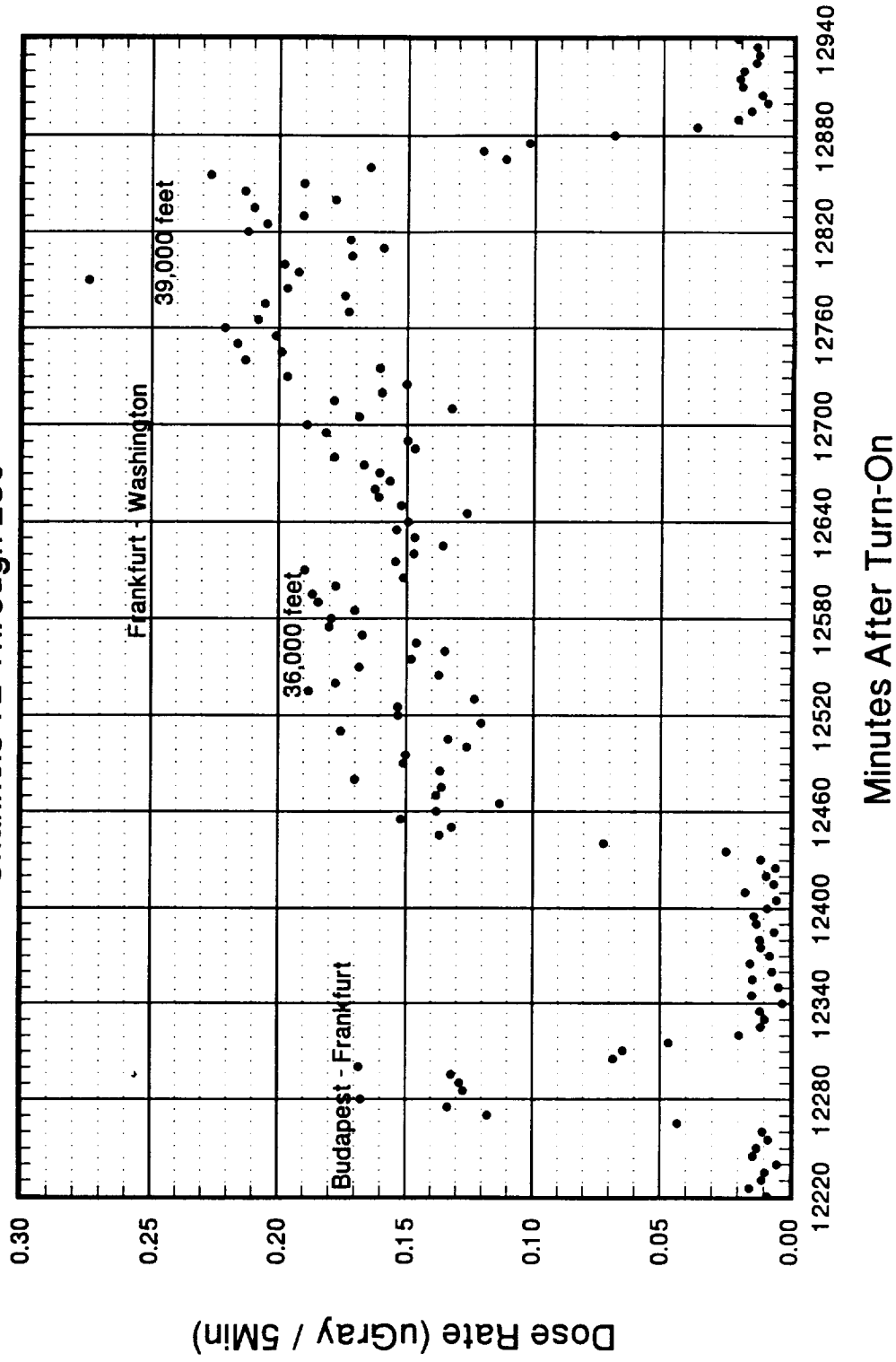


FIGURE 14